Research Article

Mahdi O. Karkush*, Majeed R. Sabaa, Alaa D. Salman, and Ayad Al-Rumaithi

Prediction of bearing capacity of driven piles for Basrah governatore using SPT and MATLAB

https://doi.org/10.1515/jmbm-2022-0005
Received Jan 17, 2022; accepted Feb 28, 2022

Abstract: Based on the results of standard penetration tests (SPTs) conducted in Al-Basrah governorate, this research aims to present thematic maps and equations for estimating the bearing capacity of driven piles having several lengths. The work includes drilling 135 boreholes to a depth of 10 m below the existing ground level and three standard penetration tests (SPT) at depths of 1.5, 6, and 9.5 m were conducted in each borehole. MATLAB software and corrected SPT values were used to determine the bearing capacity of driven piles in Al-Basrah. Several-order interpolation polynomials are suggested to estimate the bearing capacity of driven piles, but the first-order polynomial is considered the most straightforward. Furthermore, the root means squared error (RMSE) for all suggested polynomials are roughly the same. The production of thematic maps demonstrates the variation in bearing capacity of driven piles over the entire territory of Al-Basrah governorate in correlation with different depths. The results of the statistical equations showed that there is good agreement with those obtained from the SPT data. When compared with the observed values from SPT, the allowable bearing capacity results for the driven piles ranged from (−3 to +38)%. The main results of this study showed a variation of 30% between calculated and estimated values of bearing capacity of driven piles for all lengths of piles at a 95% confidence interval.

Keywords: driven pile, standard penetration test, bearing capacity, stochastics, Basrah city, MATLAB

***Corresponding Author: Mahdi O. Karkush:** Civil Engineering Department, University of Baghdad, Baghdad, Iraq; Email: mahdi_karkush@coeng.uobaghdad.edu.iq
Majeed R. Sabaa: Construction and Building Department, Al-Furat Al-Awsat University, Babylon, Iraq
Alaa D. Salman: Surveying Engineering Department, University of Baghdad, Baghdad, Iraq
Ayad Al-Rumaithi: Civil Engineering Department, University of Baghdad, Baghdad, Iraq

1 Introduction

One of the most prevalent and commonly utilized tests in geotechnical engineering is the standard penetration test. The results of this test are considered a good indicator for soil geotechnical parameters like density, shear strength, and compressibility. For earthquake planning, the SPT can be used to determine the liquefaction risk of saturated granular soils. As a result of its simplicity, low cost, and widespread availability of SPT equipment, SPT results have been accepted for the preliminary design of foundations [1–3]. Before using the measured N-values to estimate and calculate soil geotechnical parameters, they must undergo a series of adjustments. In order to get more reliable results, the corrected N-value should be taken into account. Several studies have recommended using these corrections to eliminate measurement N-value uncertainty based on their findings, but selecting the correct modifications is critical to avoid the need for additional field measurements or lab calculations [3–5].

Furthermore, the field conditions, the size and characteristics of test equipment, and the diameter and depth of boreholes all play a role in optimizing selected corrections. All of these corrections should be investigated by the geotechnical engineer. Several studies have found that corrected SPT values are related to the soil geotechnical parameters such as shear strength, density, body wave velocities, and liquefaction potential. However, such parameters are still deemed preliminary and cannot be used in the detailed design of foundations. The statistical tests can be used to demonstrate a correlation between the findings of SPTs and the results of other potential field tests such as cone penetration test and pressure meter test, which approves the findings of SPTs [6–12].

The main goal of study is to create thematic maps that show the differences in bearing capacity of driven piles concerning their geographic locations and length. MATLAB software was used to perform several regression analyses producing 1st, 2nd, 3rd, and 4th order polynomials based on the results of SPTs carried out in 135 boreholes drilled to a depth of 10 meters below current ground level and distributed over the entire area of Al-Basrah governorate.

The findings of the study provide a simple and rapid test for calculating the bearing capacity of driven piles, which can be used directly in the preliminary design of foundation or even in the detailed design of foundations for small projects or temporary works [13–17].

2 Corrections of standard penetration test

The standard penetration test (SPT) is one of the common field tests suggested for various soil types, especially when sampling and laboratory testing are problematic. The SPT value (N-value) is the number of blows on a split spoon sampler that penetrates 300 mm in the soil. The measured N-value must be subject to several corrections to comply with the standard testing process before it can be used to interpret SPT results [18]. A variety of factors can influence the measured N-values from SPTs. These factors have the potential to increase or reduce N-values, which will have a substantial impact on the soil's predicted geotechnical properties. The geotechnical properties of soil estimated from the SPT values are mostly underestimation, which means a conservative property of soil will be obtained from SPT results. As a result, many modifications to the SPT values may be done to make them more accurate, resulting in more reliable and widely accepted geotechnical properties of soil estimated using SPT data [19].

The depth and diameter of boreholes, type of hammer, diameter of drilling rod, and field parameters such as confining pressure and groundwater table (GWT) can influence the corrections. According to Fletcher [20], the following factors can influence the measured N-values:

- Variation in the weight of hammer and height of drop;
- Using heavy drill rods with a diameter greater than 1 inch;
- The length of the drilling rod exceeds 50 m;
- Using a damaged split spoon sampler;
- Failure to place the sampler on undisturbed soil;
- Careless in counting the number of blows.

In empirical correlations, the geotechnical and geophysical properties of soil are assessed using corrected SPT values ($N_{1(60)}$) [21]. Eq. (1) indicates the necessary corrections that must be considered to the measured blow count to produce the corrected SPT values ($N_{1(60)}$).

$$N_{1(60)} = N \cdot C_W \cdot C_N \cdot C_E \cdot C_B \cdot C_R \quad (1)$$

Where
$N_{1(60)}$ – corrected SPT value for the theoretical free-fall hammer with 60% energy;
N – SPT value measured in the field;
C_N – overburden pressure correction factor;
C_E – correction factor for transmitted energy to the SPT stem;
C_W – correction factor for the GWT;
C_B – correction factor for the diameter of the borehole;
C_R – The length of SPT stem correction factor.

For rod lengths greater than 6 m, the rod correction factor (C_R) can be taken unity; for rod lengths less than 3 m, C_R = 0.75 is recommended. In this investigation, C_R is set to unity to keep things simple [17]. In boreholes larger than 12 cm in diameter, the borehole diameter adjustment should be considered, but the diameter of the drilling in this study was 10 cm, so the correction factor (C_B) is set to unity. The measured N-value decreases as the confining pressure decreases due to increasing the borehole diameter. It's worth mentioning that many of these considerations are overlooked during site studies [1–4].

2.1 Effect of groundwater

A linear interpolation correction factor (C_w) was suggested by Peck *et al.* [19] to correct the SPT value for the groundwater effect. The creation of upward seepage pressure and soil bed disruption caused by groundwater entering from the borehole's bottom should be avoided in general. When the SPT is carried out below the GWT, the measured N-value can be corrected further; this correction is made if N is more than 15, and the soil resistance increases due to the negative excess pore water pressure generated during the SPT period [22].

$$N' = 15 + \frac{1}{2}(N - 15) \quad \text{for } N > 15 \quad (2)$$

Where
N' – the SPT value corrected for the GWT.

2.2 Confining pressure correction (C_N)

Due to the increasing confinement of the overlying soils, standard penetration tests conducted at significant depths in a homogeneous soil deposit will yield higher N-values than shallow tests (effective vertical stresses rise with depth). As a result, the field N-value is normalized to 100 kPa reference stress at any depth using the overburden stress correction. The overburden pressure correction factor, which is utilized for soils with a relative density of 40 to 60%, can be calculated using Eq. (3) [17].

$$C_N = \frac{200}{100 + \sigma'_o} \quad (3)$$

where σ'_o is the effective overburden pressure in kPa. The soil's saturated and dry unit weights are 17 kN/m^3 and 15 kN/m^3, respectively, because the soil layers at all investigated sites vary from soft clay to silty clay.

2.3 Energy correction (C_E)

The energy correction is used to account for different types of hammer testing (e.g., safety, donut, and automatic). The SPT stem receives around 60% of the maximum free-fall energy delivered by the safety hammer. The automated hammer delivers 95 to 100% of the maximum free fall energy to the SPT stem, whereas the donut hammer delivers 45%. The energy correction factor (C_E) is equivalent to 0.8–1.0 in the literature. To account for the hammer's verticality and free fall distance, the energy correction factor is calculated to 0.6 in this study [19, 22].

3 Description of study area and field tests

The study area is the governorate of Al-Basrah, which was established in 636 AD and is located in southern Iraq at 30° 30′ 29.1672″ N and 47° 47′ 0.5604″ E on the Global Positioning System (GPS). This city is home to Iraq's main port, Um Qasar, and numerous oil wells. The prominence of Al-Basrah governorate stems from the city's oil fields and construction one of Al-Faw port on the Arabian Gulf to the south. Boreholes were drilled to a depth of 10 meters below ground level, with a ground surface elevation of approximately 5 meters above sea level. Boreholes were drilled throughout the study area, particularly along the two sides of the Shatt Al-Arab River, which runs northwest to southeast through the city.

The quality and level of groundwater table significantly impact the magnitude of allowable bearing capacity of driven piles. The fieldwork had been conducted over a large area of Al Basrah governorate; the drilled boreholes were mostly conducted in available free lots, which reflected the nonuniform distribution of boreholes in the study area.

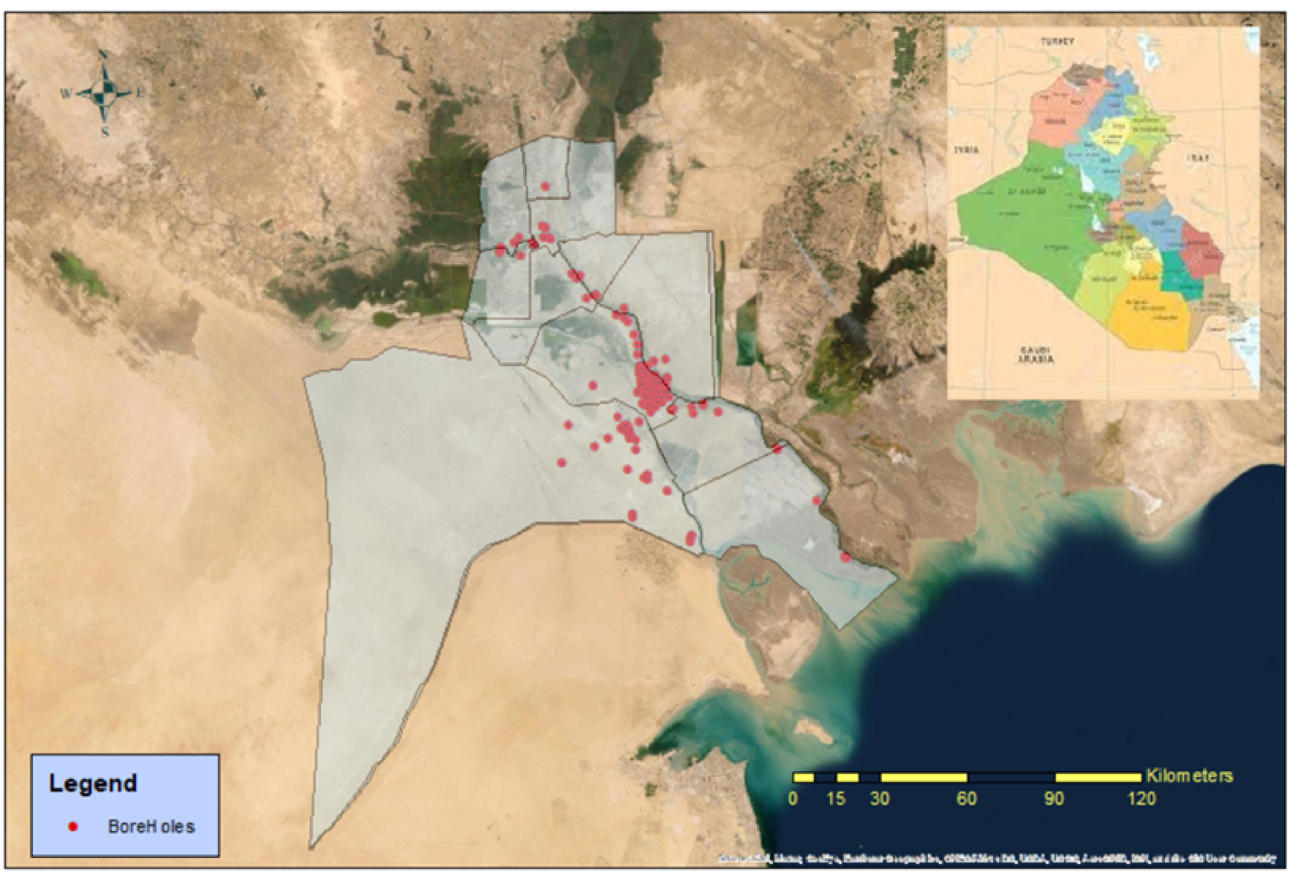

Figure 1: Distribution of the boreholes (source: Google Maps)

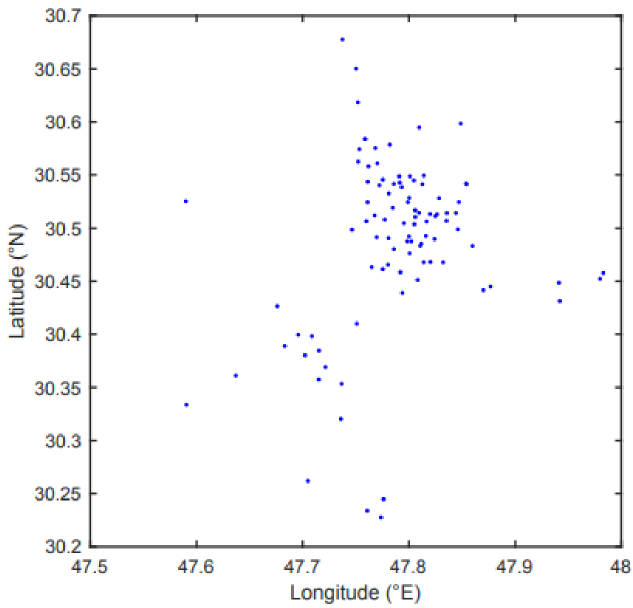

Figure 2: Borehole locations used in the analysis

Also, boreholes must be drilled in undeveloped properties to prevent conflicts with property owners and the restricted space available in the built area. To avoid any issues during drilling, the crew began by locating existing facilities such as sewage pipes, electrical cables, freshwater pipelines, and telephone, and internet connections within the study area. The boreholes were drilled with a flying auger with a diameter of 10 cm and extended to a depth of 10 m below ground level. Several SPTs were performed using an automatic hammer along the depth of boreholes.

On a Google Earth satellite view, Figure 1 shows drilled boreholes' distribution. In addition, Figure 2 shows the study area and distribution of boreholes. The SPTs data were used to compute the driven pile's permitted bearing capacity. Furthermore, after 24 hours of drilling, the GWT was measured in the field, and the density of the soil was calculated experimentally for each well. Because the groundwater level in some boreholes had not risen after 24 hours, the GWT has no value in Table 1 and has no bearing capacity calculation impact. Table 1 shows the measured N-values from SPTs conducted at depths of 1.5, 6, and 9.5 m below the existing ground surface, as well as the GWT for 135 boreholes. Due to the highly soft soil layers at those depths, conducting successful SPTs in some boreholes and at specific depths, such as boreholes 80 and 84 in Table 1, is difficult.

4 Bearing capacity of driven piles

Predicting the bearing capacity of piles is one of the difficult tasks in geotechnical engineering. Therefore several strategies and approaches have been developed to overcome forecast uncertainty. Certain simplifying assumptions and/or empirical methodologies are used in the procedures for soil stratigraphy, soil-pile structural interaction, and soil resistance distribution along the pile. As a result, they are unable to generate fully quantitative results that may be applied directly to foundation design. Five approaches for determining pile bearing capacity can be used:

- In-situ dynamic testing.
- In-situ static testing.
- In-situ integrity testing.
- Theoretical calculation of bearing capacity of piles based on soil properties and pile type and dimensions.
- Indirect methods based on the results of in-situ investigation tests [3, 23–25].

In recent years, in-situ testing approaches have grown rapidly in the geotechnical design of piles foundations. This is due to the rapid development of in-situ testing devices, a better understanding of soil behavior, and an awareness of some of the limitations and shortcomings of traditional laboratory testing. There are two methods for estimating or calculating the bearing capacity of a pile: direct and indirect ways. The use of pile-load tests and theoretical computations are examples of direct approaches. The SPT is one of the indirect approaches used to assess the pile bearing capacity in this study. Filtering and averaging data of pile resistance, failure zone around the pile base, total stress approaches, and pile capacity in dense strata with restricted base penetration are all factors that influence the uncertainty of indirect methods. The bearing capacity of driven piles estimatedfrom the results of corrected SPT values is nearly equivalent to those calculated from static testing [26–29].

The total number of drilled boreholes was 135; however, only 95 boreholes were chosen in this investigation to reduce numerical dispersion caused by significant changes in SPT values in certain places, which affected the reliability of the MATLAB software results. The bearing capacity of driven piles was evaluated for 95 boreholes drilled to a depth of 10 m below ground level and spread across the entire study area of Al-Basrah governorate. The bearing capacity of driven piles with lengths 6, 7, 8, 9, and 10 m estimated from polynomials generated using MATLAB were compared with those obtained from empirical equations based on corrected SPT values. When calculating the allowable bearing capacity of driven piles, a high safety factor of 3 is considered due to the soil's heterogeneity, high variation in GWT, and high quantities of organic matter and garbage.

The main changes to the SPT values were the overburden correction factor (C_N), as mentioned in Eq. (4), the energy correction factor (C_E), which is equivalent to 0.7, and the groundwater correction factor (C_W), as defined in Eq. (2). The corrected N-values can be used to compute the allowable bearing capacity of driven piles [26, 27]. Table 2 shows the borehole coordinates and the computed allowed bearing capacity of driven piles using Eqs. (4) to (7) with a safety factor of 3. Due to a large amount of space required to show such data, the enormous amount of data used in calculating the ultimate bearing capacity for different depths in 95 boreholes will not be shown in this study.

$$Q_b\,(kN) = 19.7 P_a A_p\,(N_{60})^{0.36} \tag{4}$$

$$Q_s\,(kN) = 0.224 P_a p L (N_{60})^{0.29} \tag{5}$$

$$Q_{ult} = Q_b + Q_s \tag{6}$$

$$Q_{all} = Q_{ult}/FS \tag{7}$$

Where
Q_b – end bearing resistance;
Q_s – skin friction resistance;
P_a – atmospheric pressure (≈ 100 kN);
A_b – cross-sectional area of pile;
P – pile perimeter;
L – pile length;
Q_{utl} – ultimate bearing capacity;
Q_{all} – allowable bearing capacity;
FS – factor of safety = 3

5 MATLAB Modeling of SPT Data

To produce a surface indicating the variance in the allowable bearing capacity of driven piles of several depths in the research region, MATLAB was used to process the data of SPTs conducted in 135 boreholes. Because of the high variance and may be singularities in the results of SPTs conducted at several depths in 135 boreholes, it's important to avoid using extreme SPT values when calculating the allowable bearing capacity of driven piles with MATLAB. These extremes could be the consequence of a small number of boreholes being drilled in particular sections of the study area or a large difference in the geotechnical properties of soil in some locations of the study area.

Several trials were conducted using the 1st order surface, 2nd order surface, 3rd order surface, and 4th order surface to develop an acceptable surface representative for the

Table 1: Coordinates, GWT, and measured SPT-value of boreholes

B.H	GPS coordinates		GWT	N-Value			B.H	GPS coordinates		GWT	N-Value		
	Latitude degree	Longitude degree	(m)	1.5 m	6 m	9.5 m		Latitude degree	Longitude degree	(m)	1.5 m	6 m	9.5 m
1	30.46324	47.76481	1.2	2	2	2	69	30.984759	47.3323	0.9	2	2	2
2	30.677667	47.737333	0.5	3	2	2	70	30.457774	47.983043	0.5	5	2	2
3	30.353224	47.736546	1	10	20	50	71	30.945994	47.270258	1	6	2	2
4	30.866987	47.548848	1	7	2	2	72	30.357404	47.715029	1	6	25	50
5	30.943651	47.263842	2.25	7	2	2	73	30.985692	47.422968	1	2	2	2
6	30.498979	47.846098	1.25	23	5	2	74	30.513353	47.819846	1	10	2	2
7	30.452369	47.979893	2.1	4	2	6	75	30.532567	47.780909	1.2	8	2	2
8	30.384517	47.715239	–	41	33	28	76	30.32028	47.73586	–	23	29	34
9	30.65027	47.750105	0.25	2	2	2	77	30.42647	47.67592	–	19	16	10
10	30.97454	47.31532	2	10	7	2	78	30.36121	47.63705	1	22	26	40
11	31.01347	47.427324	1.5	10	8	2	79	30.46789	47.83228	2	3	3	2
12	30.929563	47.337608	1	2	2	2	80	30.52529	47.59003	0.5	–	-	6
13	30.618512	47.751902	3	8	4	2	81	30.743122	47.678118	2	2	2	2
14	30.802983	47.608714	2	7	2	2	82	30.05258	47.92583	0.5	2	2	2
15	30.5068	47.835369	1.2	4	2	2	83	30.24478	47.77606	–	31	29	27
16	30.492526	47.815992	0.5	4	4	2	84	30.40101	47.49674	0.5	–	41	43
17	30.561206	47.770233	0.75	6	4	2	85	30.575532	47.76834	1.5	2	2	2
18	30.511275	47.824614	2	8	4	2	86	30.04477	47.91889	1.5	2	2	2

Table 1: ...continued

B.H	GPS coordinates		GWT	N-Value			B.H	GPS coordinates		GWT	N-Value		
	Latitude degree	Longitude degree	(m)	1.5 m	6 m	9.5 m		Latitude degree	Longitude degree	(m)	1.5 m	6 m	9.5 m
19	30.549429	47.813952	1.2	3	3	4	87	30.19468	47.84551	–	15	24	34
20	30.519017	47.784783	1	10	10	2	88	30.49137	47.7696	1.5	8	4	2
21	30.503642	47.805022	1.95	8	3	7	89	30.43096	48.03027	2.5	2	2	2
22	30.5143	47.844199	1.2	2	2	2	90	29.582635	48.27309	1.25	2	2	2
23	30.451235	47.808062	0.25	7	3	3	91	30.487565	47.802265	1.5	8	2	3
24	30.476148	47.80068	1.25	6	2	3	92	30.43907	47.793667	0.5	3	2	3
25	30.398134	47.708611	1.5	14	18	35	93	30.498611	47.746389	0.5	2	2	2
26	30.524343	47.761026	1.5	8	4	3	94	30.558264	47.761877	0.5	2	2	2
27	30.542873	47.791312	1.5	12	6	3	95	30.410137	47.750771	–	11	19	30
28	30.545661	47.775351	2.1	8	2	5	96	30.548722	47.790806	0.75	8	3	3
29	30.528592	47.800295	0.8	9	6	3	97	30.483453	47.810493	1.5	8	2	5
30	30.444847	47.876889	1.2	2	2	2	98	30.511952	47.767686	1.5	8	4	4
31	30.562611	47.752161	1.8	7	2	2	99	30.514264	47.835641	1.2	8	5	3
32	30.46125	47.775306	1.0	6	2	3	100	30.504509	47.795087	0.95	8	2	2
33	30.492161	47.8001	1.4	10	4	3	101	30.468246	47.820135	2.1	18	13	2
34	30.528288	47.828266	1.25	8	7	11	102	30.380307	47.702145	10	34	38	35
35	30.542023	47.853618	0.25	7	6	4	103	30.759306	47.7045	0.25	6	2	2
36	30.490531	47.780647	1.63	8	4	4	104	30.261936	47.704736	–	9	10	17
37	30.574453	47.753307	0.5	6	2	2	105	30.485403	47.811495	1	4	3	2
38	30.388941	47.683118	1.0	12	25	50	106	30.467966	47.813826	0.6	4	4	2
39	30.5079	47.777086	0.5	8	3	3	107	30.465589	47.780119	2.1	8	3	3
40	30.369006	47.721302	10	13	18	26	108	30.28501	47.47257	1.2	8	2	3
41	30.448513	47.941167	3.5	5	2	2	109	30.543719	47.761162	2.2	8	3	4
42	30.516736	47.805846	0.9	8	2	3	110	30.315603	48.242598	2.5	2	2	2
43	30.79525	47.573028	0.25	2	2	2	111	30.541672	47.785828	0.7	9	6	5
44	30.545003	47.804686	0.5	6	3	4	112	30.538565	47.793098	1	10	4	2
45	30.123251	47.71726	–	50	45	42	113	30.548753	47.800998	1.1	7	6	4
46	30.506425	47.759875	0.5	4	4	6	114	30.524387	47.798975	1.1	4	4	2
47	29.973944	48.468417	–	2	2	2	115	30.578647	47.781908	1	2	2	2
48	30.719042	47.718392	1.25	6	2	2	116	30.524472	47.847061	1	6	4	2
49	30.594667	47.809473	2.1	10	8	2	117	30.114687	47.715509	–	50	48	46
50	30.458433	47.791947	1.2	4	2	4	118	30.233761	47.760731	1	46	40	35
51	30.98478	47.44377	1.0	8	7	2	119	29.971258	48.476035	1	2	2	2
52	30.489653	47.823968	3	8	3	4	120	30.44163	47.869875	2.2	6	2	2
53	30.483358	47.859833	2.1	2	2	2	121	30.732536	47.703688	1.25	6	2	2
54	30.399438	47.695805	–	33	22	35	122	30.805461	47.601909	2	6	2	2
55	30.33382	47.59058	–	50	45	42	123	30.855089	47.53756	2	2	2	2
56	30.506131	47.816672	2.1	8	2	5	124	30.981152	47.449086	0.25	7	2	2
57	30.3117	48.24045	1.5	2	2	2	125	30.971853	47.382546	0.25	2	2	2
58	31.020338	47.416235	1	8	2	2	126	30.956501	47.271284	0.25	4	2	2
59	30.431172	47.942036	4	2	2	2	127	31.015355	47.429864	0.5	8	2	6
60	30.583858	47.758782	3.2	12	8	2	128	31.144262	47.43092	2.5	2	7	2
61	30.032503	47.919989	2.5	19	23	14	129	30.149344	48.373275	1	2	2	2
62	30.22773	47.773719	–	29	25	30	130	30.513148	47.82633	1.25	4	2	2
63	30.963884	47.387458	2.6	10	2	2	131	30.541316	47.812604	1.5	7	2	2
64	30.541292	47.854056	2.1	5	10	2	132	30.510489	47.805907	2	3	2	4
65	30.540332	47.772309	1.2	10	4	5	133	30.5145	47.80936	0.5	3	3	3
66	30.870981	47.52157	1.25	2	2	2	134	30.598381	47.848881	1	5	2	2
67	30.583779	47.75878	1.25	5	2	2	135	30.4876	47.7983	2.1	14	3	2
68	30.480276	47.785883	0.5	8	5	5	–	–	–	–	–	–	–

Table 2: Corrected SPT values and allowable bearing capacity of driven piles

BH	Length (m)	$N_{1(60)}$	Q_b kN	Q_s kN	Q_{ult} kN	Q_{all} kN	BH	Length (m)	$N_{1(60)}$	Q_b kN	Q_s kN	Q_{ult} kN	Q_{all} kN
	6		202.50	185.22	387.71	129.24		6		460.10	358.76	818.87	272.96
	7		202.50	216.09	418.58	139.53		7		460.10	418.56	878.66	292.89
1	8	1.92	202.50	246.96	449.45	149.82	83	8	18.80	460.10	478.35	938.45	312.82
	9		202.50	277.82	480.32	160.11		9		460.10	538.15	998.25	332.75
	10		202.50	308.69	511.19	170.4		10		460.10	597.94	1058.04	352.68
	6		379.03	306.90	685.94	228.65		6		273.59	236.02	509.61	169.87
	7		379.03	358.05	737.09	245.70		7		273.59	275.36	548.95	182.98
6	8	10.97	379.03	409.21	788.24	262.75	91	8	4.44	273.59	314.69	588.28	196.09
	9		379.03	460.36	839.39	279.80		9		273.59	354.03	627.62	209.21
	10		379.03	511.51	890.54	296.85		10		273.59	393.37	666.96	222.32
	6		278.04	239.11	517.15	172.38		6		284.79	243.78	528.57	176.19
	7		278.04	278.96	557.00	185.67		7		284.79	284.41	569.20	189.73
18	8	4.64	278.04	318.81	596.85	198.95	97	8	4.96	284.79	325.04	609.83	203.28
	9		278.04	358.66	636.70	212.23		9		284.79	365.67	650.46	216.82
	10		278.04	398.51	676.55	225.52		10		284.79	406.30	691.09	230.36
	6		202.50	185.22	387.71	129.24		6		238.87	211.58	450.45	150.15
	7		202.50	216.09	418.58	139.53		7		238.87	246.84	485.71	161.90
30	8	1.92	202.50	246.96	449.45	149.82	105	8	3.04	238.87	282.11	520.98	173.66
	9		202.50	277.82	480.32	160.11		9		238.87	317.37	556.24	185.41
	10		202.50	308.69	511.19	170.40		10		238.87	352.63	591.50	197.17
	6		390.14	314.13	704.27	234.76		6		320.23	267.93	588.16	196.05
	7		390.14	366.48	756.62	252.21		7		320.23	312.59	632.81	210.94
40	8	11.89	390.14	418.84	808.98	269.66	111	8	6.87	320.23	357.24	677.47	225.82
	9		390.14	471.19	861.33	287.11		9		320.23	401.90	722.12	240.71
	10		390.14	523.55	913.69	304.56		10		320.23	446.55	766.78	255.59
	6		244.04	215.26	459.31	153.10		6		245.31	216.16	461.47	153.82
	7		244.04	251.14	495.19	165.06		7		245.31	252.19	497.50	165.83
50	8	3.23	244.04	287.02	531.06	177.02	120	8	3.28	245.31	288.22	533.52	177.84
	9		244.04	322.90	566.94	188.98		9		245.31	324.24	569.55	189.85
	10		244.04	358.77	602.82	200.94		10		245.31	360.27	605.58	201.86
	6		319.50	267.44	586.94	195.65		6		228.59	204.22	432.81	144.27
	7		319.50	312.01	631.51	210.50		7		228.59	238.25	466.84	155.61
60	8	6.83	319.50	356.59	676.09	225.36	130	8	2.69	228.59	272.29	500.88	166.96
	9		319.50	401.16	720.66	240.22		9		228.59	306.32	534.91	178.30
	10		319.50	445.73	765.23	255.08		10		228.59	340.36	568.95	189.65
	6		243.86	215.14	459.00	153.00		6		237.74	210.77	448.51	149.50
	7		243.86	250.99	494.85	164.95		7		237.74	245.90	483.63	161.21
70	8	3.22	243.86	286.85	530.71	176.90	133	8	3.00	237.74	281.03	518.76	172.92
	9		243.86	322.70	566.57	188.86		9		237.74	316.16	553.89	184.63
	10		243.86	358.56	602.42	200.81		10		237.74	351.28	589.02	196.34
	6		244.59	215.65	460.24	153.41		6		314.31	263.94	578.25	192.75
	7		244.59	251.59	496.18	165.39		7		314.31	307.93	622.24	207.41
77	8	3.25	244.59	287.53	532.12	177.37	135	8	6.52	351.92	351.92	351.92	222.08
	9		244.59	323.48	568.06	189.35		9		314.31	395.91	710.22	236.74
	10		244.59	359.42	604.00	201.33		10		314.31	439.90	754.21	251.40

Table 3: Parameters of suggested polynomials were used to determine the allowable bearing capacity of 6 m length driven piles

Fit Order	Number of terms	Sum of square errors (SSE), kN	R^2	Decision feedback equalizer (DFE)	Adjusted R^2	RMSE, kN
1	3	7.2287e+04	0.6379	89	0.6175	28.4993
2	6	6.2497e+04	0.6869	85	0.6537	27.1157
3	10	6.2497e+04	0.6869	85	0.6537	27.1157
4	15	0.8606e+04	0.7565	80	0.7139	24.6491

Table 4: Parameters defing four polynomials suggested for caluculations of the allowable bearing capacity driven pile of 6 m length

Factor	First-order model			Second-order model			Third-order model			Fourth-order model		
	Min.	Max.	Av.	Min.	Max.	Av.	Min.	Max.	Av.	Min.	Max.	Av.
P_{00}	312.1	379	345.5	422	657	539.5	−160.1	457.4	148.7	−2256	303.6	−976.1
P_{10}	−343.2	−137	−240.1	−1377	−239.9	−808.6	−1616	3075	729.5	−6334	14560	4116
P_{01}	−405.8	−248.9	−327.3	−1943	−923.3	−1433	2253	5019	2253	6334	35050	20710
P_{20}	-	-	-	−1119	316.7	−401.3	−10210	5372	−2419	−34660	52770	9054
P_{11}	-	-	-	1737	4875	3306	−15620	3372	−6123	−199900	40910	−79500
P_{02}	-	-	-	−50.6	1059	504.1	−16740	−2197	−9470	−138600	56960	−97780
P_{30}	-	-	-	-	-	-	−1068	12310	5623	−169900	69220	−50320
P_{21}	-	-	-	-	-	-	−26790	7554	−9618	−195100	351900	78370
P_{12}	-	-	-	-	-	-	7676	48710	28200	39580	496800	268200
P_{03}	-	-	-	-	-	-	−1458	8410	3476	71280	261700	166500
P_{40}	-	-	-	-	-	-	-	-	-	−12940	172800	79950
P_{31}	-	-	-	-	-	-	-	-	-	−416500	131200	−142700
P_{22}	-	-	-	-	-	-	-	-	-	−545100	639600	47240
P_{13}	-	-	-	-	-	-	-	-	-	−599200	−140400	−369800
P_{04}	-	-	-	-	-	-	-	-	-	−1.20500	−11390	−6.5930

fluctuation of bearing capacity of driven piles having several lengths with spatial coordinates. The bearing capacity of driven piles from produced surfaces can be calculated using Eqs. (8) to (11). Tables 3 and 4 contain the corresponding parameters for each equation. More accurate findings are obtained by increasing the order of the polynomial representing the surface depicting the fluctuation of the bearing capacity of driven piles. However, such a surface will increase the number of parameters required to compute the bearing capacity, making the procedure more difficult. The number of parameters increases from three to fifteen when the polynomial order is changed from first to fourth, as shown in Table 3, while the root means square error (RMSE) remains unchanged. Figures 3 to 6 illustrate the surfaces created using 1st, 2nd, 3rd, and 4th order polynomials for variation in bearing capacity of a driven pile of 6 m length for 95 boreholes.

The first- and second-order interpolation polynomials almost invariably result in flat surfaces, which essentially reflect variations in the allowable bearing capacity as a function of coordinates and length. Furthermore, while applying the equation with less parameters is simple, employing third- and fourth-order interpolations will result in surfaces with several folds, resulting in extremely sensitive estimates of the allowable bearing capacity of driven piles, especially around inflection point surfaces. As a result, adopting 1st-order interpolation, where the surface polynomial has just three parameters and an acceptable root mean squared error (RMSE) when predicting the allowed bearing capacity of driven piles, is advised to save time and effort. R^2 is also the fraction of the dependent variable's variation that can be predicted by the independent variable(s), and it ranges from 0.6379 to 0.7565. As the order of the polynomial used to represent experimental data increased, the value of R^2 increased. This was due to a closer match between the pile's projected allowed bearing capacity and determined SPT values. The adjusted R^2 is a type of R^2 that has been adjusted to account for the model's number of predictors.

The 1st order polynomial with 95% confidence bounds is:

$$Q_{all}(kN) = P_{00} + P_{10} * X + P_{01} * Y \tag{8}$$

The 2nd order polynomial with 95% confidence bounds is:

$$Q_{all}(kN) = P_{00} + P_{10} \cdot X + P_{01} \cdot Y + P_{20} \cdot X^2 + P_{11} \cdot X \cdot Y + P_{02} \cdot Y \tag{9}$$

The 3rd order polynomial with 95% confidence bounds is:

$$Q_{all}(kN) = P_{00} + P_{10} \cdot X + P_{01} \cdot Y + P_{20} \cdot X^2 + P_{11} \cdot X \cdot Y + P_{02} \cdot Y^2 + P_{30} \cdot X^3 + P_{21} \cdot X^2 \cdot Y + P_{12} \cdot X \cdot Y^2 + P_{03} \cdot Y^3 \quad (10)$$

The 4th order polynomial with 95% confidence bounds is:

$$Q_{all}(kN) = P_{00} + P_{10} \cdot X + P_{01} \cdot Y + P_{20} \cdot X^2 + P_{11} \cdot X \cdot Y + P_{02} \cdot Y^2 + P_{30} \cdot X^3 + P_{21} \cdot X^2 \cdot Y + P_{12} \cdot X \cdot Y^2 + P_{03} \cdot Y^3 + P_{40} \cdot X^4 + P_{31} \cdot X^3 \cdot Y + P_{22} \cdot X^2 \cdot Y^2 + P_{13} \cdot X \cdot Y^3 + P_{04} \cdot Y^4 \quad (11)$$

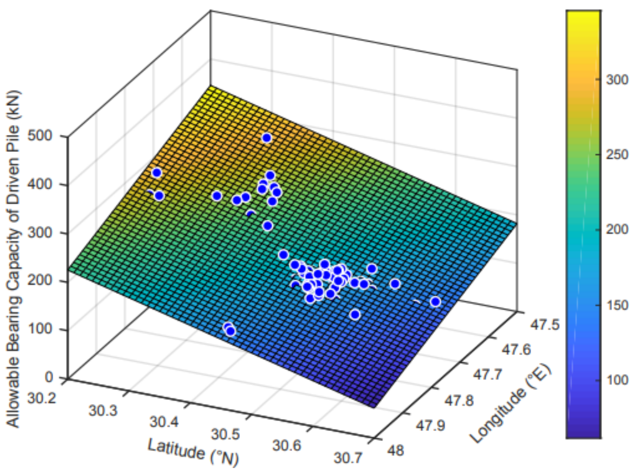

Figure 3: Variation of the allowable bearing capacity of driven piles (6 m length) using 1st order polynomial

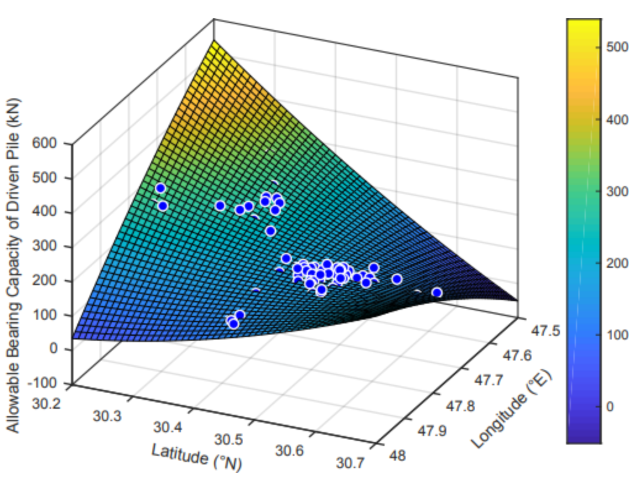

Figure 4: Variation of the allowable bearing capacity of driven piles (6 m length) using 2nd order polynomial

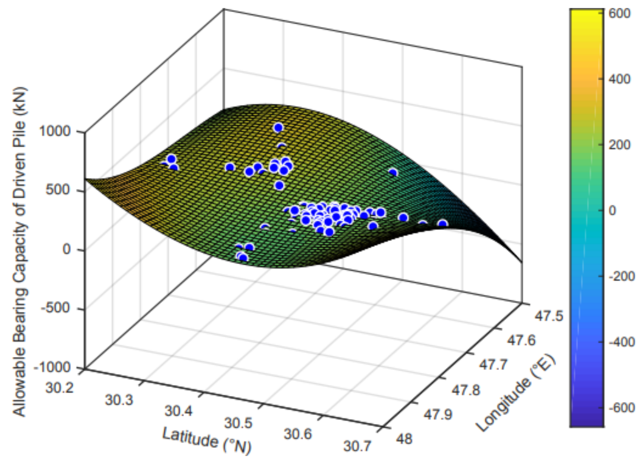

Figure 5: Variation the allowable bearing capacity of driven pile (6 m length) using 3rd order polynomial

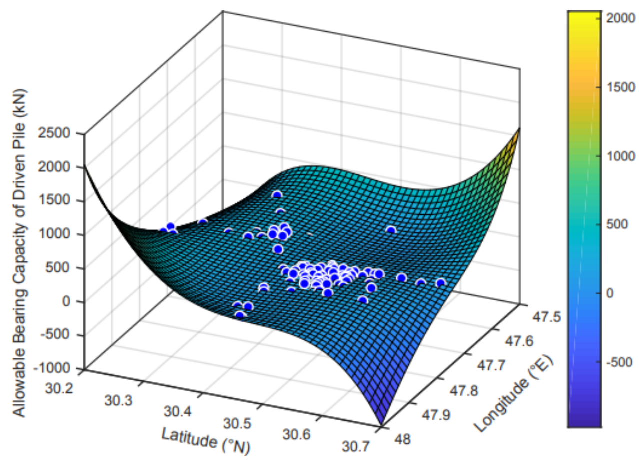

Figure 6: Variation the allowable bearing capacity of driven pile (6 m length) using 4th order polynomial

6 Results and discussion

Using the coordinates of 95 boreholes and the corrected N-values obtained from SPTs, the first-order interpolation outlined in the preceding section will be used to estimate the allowable bearing capacity of driven piles with lengths of 6, 7, 8, 9, and 10 m. The first-order polynomial in Eq. (8) will be used to determine the allowable bearing capacity of driven piles having several depths. The parameters defining the polynomial for all investigated lengths of driven piles are given in Table 5. Because of the large range of recorded SPT values, there was no uniformity in the values of a parameter defining the 1st order polynomials [3]. The SPT values generally increased with depth; however, the soft layer stratification caused the SPT values to decrease in some boreholes. To avoid the uncertainty caused by SPT values and seasonal oscillations in the GWT, the

Table 5: Parameters of 1st order polynomials used to estimate the allowable bearing capacity of piles

Length (m)	P_{00}			P_{10}			P_{01}		
	Min.	Max.	Av.	Min.	Max.	Av.	Min.	Max.	Av.
6	312.1	379	345.5	−343.2	−137	−240.1	−405.8	−248.9	−327.3
7	334.6	406	370.3	−366	−145.9	−256	−432.7	−265.3	−349
8	357	433	395	−388.8	−145.9	−271.8	−459.7	−281.7	−370.7
9	379.5	459.9	419.7	−411.6	−163.8	−287.7	−486.7	−298.1	−392.4
10	402	486.9	444.4	−434.4	−172.8	−303.6	−513.6	−314.6	−414.1

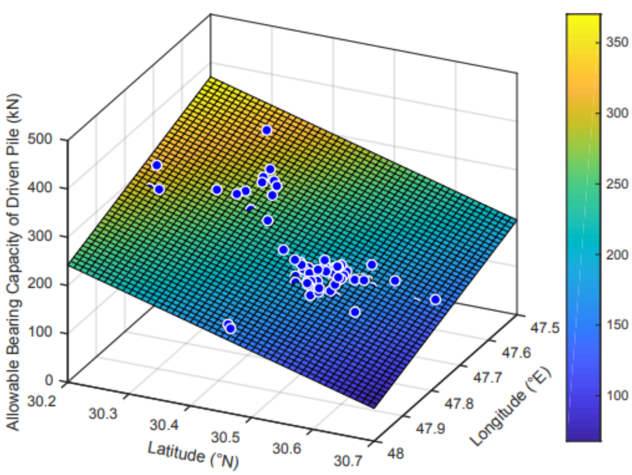

Figure 7: Surface defining the variation of the allowable bearing capacity of the driven pile having 7 m length

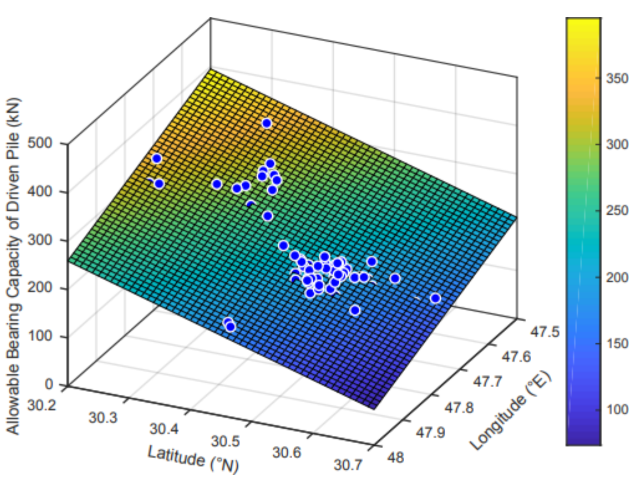

Figure 8: Surface defining the variation of the allowable bearing capacity of the driven pile having 8 m length

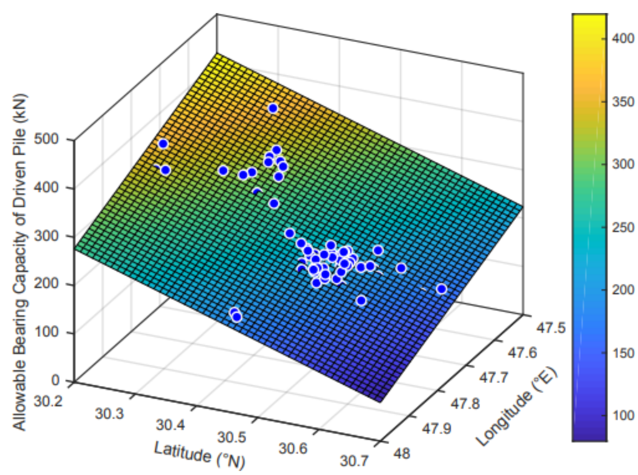

Figure 9: Surface defining the variation of the allowable bearing capacity of the driven pile having 9 m length

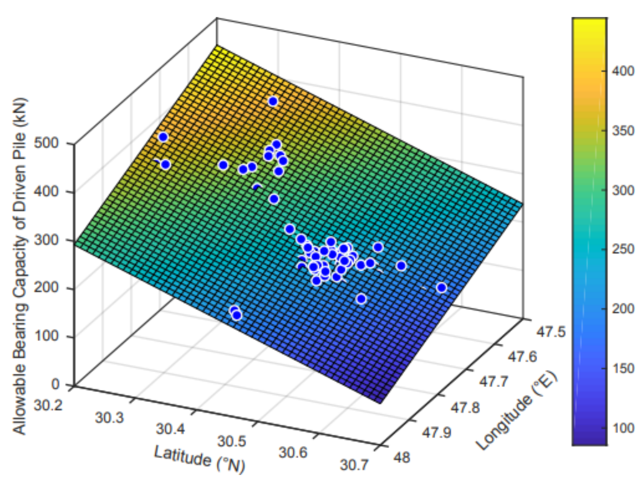

Figure 10: Surface defining the variation of the allowable bearing capacity of the driven pile having 10 m length

overburden pressure is calculated using the effective unit weight in this study. The surfaces representing the change in allowable bearing capacity of several lengths of driven piles are planes, as shown in Figures 7 to 10. The disparity revealed that the northern study area authorized bearing capacity of driven piles is higher than the southern parts of the study area. Table 6 shows comparison between the results of bearing capacity of driven piles calculated from SPTs and proposed 1st order polynomial.

Additionally, as soil depth increases, its allowable bearing capacity increases. The five depths studied all followed the same pattern. According to the allowable bearing ca-

Table 6: Comparison of allowable bearing capacity of driven piles predicated from 1st order polynomial and those calculated from SPTs

BH (No.)	Length of pile (m)	Q_{all} SPT-Test	Q_{all} 1st order model	% difference	BH (No.)	Length of pile (m)	Q_{all} SPT-Test	Q_{all} 1st order model	% difference
1	6	129.24	195.76	33.98	83	6	272.96	264.56	−3.17
	7	139.53	210.63	31.60		7	292.89	284.00	−3.13
	8	149.82	225.44	33.54		8	312.82	303.37	−3.11
	9	160.11	240.21	33.33		9	332.75	322.71	−3.11
	10	170.4	254.99	33.17		10	352.68	342.044	−3.11
6	6	228.65	164.54	−38.96	91	6	169.87	178.81	4.99
	7	245.70	177.35	−38.61		7	182.98	192.56	4.97
	8	262.75	190.09	−38.22		8	196.09	206.24	4.96
	9	279.80	202.81	−37.96		9	209.21	219.90	4.87
	10	296.85	215.51	−37.34		10	222.32	233.55	4.81
18	6	172.38	165.68	−4.06	97	6	176.19	178.17	1.15
	7	185.67	178.56	−3.99		7	189.73	191.88	1.12
	8	198.95	191.38	−3.95		8	203.28	205.53	1.09
	9	212.23	204.16	−3.83		9	216.82	219.14	1.06
	10	225.52	216.94	−3.71		10	230.36	232.75	1.03
30	6	129.24	174.87	26.09	105	6	150.15	177.30	15.31
	7	139.53	188.36	25.92		7	161.90	190.95	15.21
	8	149.82	201.79	25.66		8	173.66	204.53	15.09
	9	160.11	215.19	25.59		9	185.41	218.09	14.98
	10	170.40	228.58	25.45		10	197.17	231.65	14.88
40	6	234.76	237.04	0.96	111	6	196.05	165.04	−18.81
	7	252.21	254.66	0.96		7	210.94	177.88	−18.58
	8	269.66	272.20	0.93		8	225.82	190.65	−18.46
	9	287.11	289.71	0.89		9	240.71	203.40	−18.34
	10	304.56	307.08	0.82		10	255.59	216.14	−18.25
50	6	153.10	190.81	19.76	120	6	153.82	177.61	13.40
	7	165.06	205.36	19.62		7	165.83	191.28	13.30
	8	177.02	219.84	19.51		8	177.84	204.89	13.20
	9	188.98	234.29	19.33		9	189.85	218.47	13.10
	10	200.94	248.74	19.21		10	201.86	232.05	13.00
60	6	195.65	157.73	−24.04	130	6	144.27	164.65	12.37
	7	210.50	170.08	−23.76		7	155.61	177.47	12.31
	8	225.36	182.36	−23.57		8	166.96	190.22	12.22
	9	240.22	194.62	−23.42		9	178.30	202.93	12.14
	10	255.08	206.87	−23.26		10	189.65	215.65	12.05
70	6	153.00	145.15	−5.40	133	6	149.50	168.29	11.16
	7	164.95	156.67	−5.31		7	161.21	181.34	11.10
	8	176.90	168.15	−5.20		8	172.92	194.33	11.01
	9	188.86	179.58	−5.17		9	184.63	207.29	10.93
	10	200.81	191.00	−5.13		10	196.34	220.24	10.85
77	6	153.41	229.14	33.04	135	6	192.75	179.75	−7.23
	7	165.39	246.23	32.80		7	207.41	193.56	−7.15
	8	177.37	263.23	32.62		8	222.08	207.31	−7.12
	9	189.35	280.22	32.42		9	236.74	221.02	−7.11
	10	201.33	297.21	32.26		10	251.40	234.74	−7.09

pacity of driven piles, the weak zone is in the southeast corner of the city.

$$Q_{all}(kN) = P_{00} + P_{10}\,(E - 47.5) + p_{01}(N - 30.2) \quad (12)$$

Where $X = E{-}47.5$ and $Y = N{-}30.2$; E is longitude (easting) in degrees; N is latitude (northing) in degrees, and Q_{all} is the allowable bearing capacity of the driven pile (kPa).

7 Conclusions

Production of thematic surfaces showing the variation of bearing capacity of driven piles in Al-Basrah governorate is the main objective of this study. The thematic surfaces produced by MATLAB software depending on the results of SPTs conducted in the study area. The SPTs conducted at depth 1.5, 6, and 9.5 m in 135 boreholes drilled to a depth of 10 m. Based on the results of study, a preliminary estimation of bearing capacity of driven piles can be easily estimated from the proposed equations. The following points can be concluded from the results of this study:

- The results of SPTs conducted in the study area give a comprehensive idea about the geotechnical properties of soil in the study area and can be used safely to estimate the allowable bearing capacity of driven piles across Al-Basrah's governorate.
- In the preliminary design of piles, geotechnical parameters of the soil can be used.
- One of the promising techniques using MATLAB software to create a three-dimensional surface that illustrates the change in allowable bearing capacity of driven piles as a function of geographic coordinates and length.
- The first-order polynomial, with only three parameters and an RMSE of 28.4993 kN, was the simplest and easiest to calculate the allowable bearing capacity of driven piles.
- The allowable bearing capacity of driven piles obtained from the proposed Eq. (12) were in good agreement with those calculated from the SPT data. The difference in the allowable bearing capacity of driven piles calculated from proposed equation and those calculated from SPTs ranged from (−3%) to (+38%).
- Calculating the allowable bearing capacity of driven piles using the suggested equation will save time and money, especially for small projects.

Acknowledgement: The authors would like to thank the staff of the Civil Engineering department at the University of Baghdad for their kind help in conducting corrections and MATLAB analysis. Also, thanks to extended to the Directorate of Electricity Distribution in Al-Basrah for providing data of tests.

Funding: The authors declared no funding was received.

Author contributions: All authors have accepted responsibility for the entire content of this manuscript and approved its submission.

Conflict of interest: The authors state no conflict of interest.

References

[1] Clayton CR, Matthews MC, Simons NE. Site investigation. 2nd ed. London: Granada Publishing Ltd; 1982 Jan.
[2] Rocha BP, Giacheti HL. Site characterization of a tropical soil by in situ tests. Dyna (Medellin). 2018 Sep;85(206):211–9.
[3] Karkush MO, Ahmed MD, Sheikha AA, Al-Rumaithi A. Thematic maps for the variation of bearing capacity of soil using SPTs and MATLAB. Geosciences (Basel). 2020 Sep;10(9):329.
[4] Nixon IK. Standard penetration test State-of-the-art report. In: Verruijt A, Beringen FL, De Leeuw EH, editors. Penetration testing. London: Routledge; 1982. p. 3-22. https://doi.org/10.1201/9780203743959-2.
[5] Ghafghazi M, DeJong JT, Sturm AP, Temple CE. Instrumented Becker penetration test. II: iBPT-SPT correlation for characterization and liquefaction assessment of gravelly soils. J Geotech Geoenviron Eng. 2017 Sep;143(9):04017063.
[6] Bahmani SM, Briaud JL. Modulus to SPT blow count correlation for settlement of footings on sand. In: Hambleton JP, Makhnenko R, Budge AS, editors. Geo-Congress 2020: Foundations, Soil Improvement, and Erosion; 2020 Feb 25-28; Minneapolis (MN), USA. ASCE; 2020. p. 343-349. https://doi.org/10.1061/9780784482780.033.
[7] Rahimi S, Wood CM, Wotherspoon LM. Influence of soil aging on SPT-Vs correlation and seismic site classification. Eng Geol. 2020 Jul;272:105653.
[8] Anbazhagan P, Uday A, Moustafa SS, Al-Arifi NS. Correlation of densities with shear wave velocities and SPT N values. J Geophys Eng. 2016 Jun;13(3):320–41.
[9] Bandyopadhyay S, Sengupta A, Reddy GR. Development of correlation between SPT-N value and shear wave velocity and estimation of non-linear seismic site effects for soft deposits in Kolkata city. Geomech Geoengin. 2021 Jan;16(1):1–9.
[10] Thokchom S, Rastogi BK, Dogra NN, Pancholi V, Sairam B, Bhattacharya F, et al. Empirical correlation of SPT blow counts versus shear wave velocity for different types of soils in Dholera, Western India. Nat Hazards. 2017 Apr;86(3):1291–306.
[11] Mujtaba H, Farooq K, Sivakugan N, Das BM. Evaluation of relative density and friction angle based on SPT-N values. KSCE J Civ Eng. 2018 Feb;22(2):572–81.
[12] Karkush MO, Aljorany AN. Analytical and numerical analysis of piled-raft foundation of storage tank. InConstruction in Geotech-

nical Engineering. Singapore: Springer; 2020. p. 373–84.

[13] Liang X, Qin Z, Chen S, Wang D. CPT-SPT correlation analysis based on BP artificial neural network associated with partial least square regression. In: Hu L, Gu X, Tao J, Zhou A, editors. Proceedings of GeoShanghai International Conference: Multi-physics Process in Soil Mechanics and Advances in Geotechnical Testing. 2018 May 27-30; Shanghai, China. Springer, Singapore; 2018. p. 381-390.

[14] Anwar MB. Correlation between PMT and SPT results for calcareous soil. HBRC J. 2018 Apr 1;14(1):50-5. https://doi.org/10.1016/j.hbrcj.2016.03.001.

[15] Ferreira MQ, Tsuha CH, Schiavon JA, Aoki N. Determination of SPT end bearing and side friction resistances using static uplift tests. Geotech Test J. 2016 Aug;39(6):1040–7.

[16] Bolton Seed H, Tokimatsu K, Harder LF, Chung RM. Influence of SPT procedures in soil liquefaction resistance evaluations. J Geotech Eng. 1985 Dec;111(12):1425–45.

[17] Skempton AW. Standard penetration test procedures and the effects in sands of overburden pressure, relative density, particle size, ageing and overconsolidation. Geotechnique. 1986 Sep;36(3):425–47.

[18] Youd TL, Idriss IM. Liquefaction resistance of soils: summary report from the 1996 NCEER and 1998 NCEER/NSF workshops on evaluation of liquefaction resistance of soils. J Geotech Geoenviron Eng. 2001 Apr;127(4):297–313.

[19] Peck RB, Hanson WE, Thornburn TH. Foundation engineering. Williams & Wilkins; 1953. https://doi.org/10.1097/00010694-195304000-00012.

[20] Fletcher GF. Standard penetration test: its uses and abuses. J Soil Mech Found Div. 1965 Jul;91(4):67–75.

[21] Craig RF. Craig's soil mechanics. London: CRC Press; 2004. https://doi.org/10.4324/9780203494103.

[22] Eslami A, Fellenius BH. Pile capacity by direct CPT and CPTu methods applied to 102 case histories. Can Geotech J. 1997 Dec;34(6):886–904.

[23] Jebur MM, Ahmed MD, Karkush MO. Numerical analysis of under-reamed pile subjected to dynamic loading in sandy soil. IOP Conf Ser: Mater Sci Eng 2020;671:012084. https://doi.org/10.1088/1757-899X/671/1/012084.

[24] Bouali MF, Karkush MO, Bouassida M. Impact of wall movements on the location of passive Earth thrust. Open Geosci. 2021 Jan;13(1):570–81.

[25] AL-Shamaa MF. Sheikha AA, Karkush MO, Jabbar MS, Al-Rumaithi AA. Numerical Modeling of Honeycombed Geocell Reinforced Soil. In: Karkush MO, Choudhury D, editors. Modern Applications of Geotechnical Engineering and Construction. Singapore: Springer; 2021. p. 253–63.

[26] Bowles JE. Foundation analysis and design. 4th ed. New York: McGraw Hill; 1988.

[27] Das BM, Sivakugan N. Principles of foundation engineering. 9th ed. Boston: Cengage learning; 2018.

[28] Kulhawy FH, Trautmann CH. Estimation of in-situ test uncertainty. In: Shackelford CD, Nelson PP, Roth MJS, editors. Uncertainty in the geologic environment: From theory to practice. New York: ASCE; 1996. p. 269-286.

[29] Schnaid F, Lourenço D, Odebrecht E. Interpretation of static and dynamic penetration tests in coarse-grained soils. Géotech Lett. 2017 Jun;7(2):113–8.